A multi-objective collaborative optimization method of ship energy efficiency based on NSGA-II and TOPSIS

CrossMark

Daoyi Lu, Antong Wang, Huibing Gan*, Yuxin Su, Xuefei Ao

College of Marine Engineering, Dalian Maritime University

ARTICLE INFO

ABSTRACT

To enhance ship navigation efficiency and minimize fuel consumption and emissions, this study proposes a multi-objective energy efficiency optimization method for ships under actual operating conditions. A comprehensive mathematical model integrating ship, engine, and propeller dynamics while accounting for sea-state influences is developed and validated using experimental data. Based on this model, optimization models for propeller parameters and navigation speed are established. The Non-dominated Sorting Genetic Algorithm II (NSGA-II) is employed to generate the Pareto solution set, and the Technique for Order of Preference by Similarity to Ideal Solution (TOPSIS) approach is utilized to identify the optimal solution. The results demonstrate that optimizing propeller parameters enhances the propulsion efficiency by 2.11%, reduces the specific fuel oil consumption (SFOC) by 1.93%, and reduces the nitrogen oxide (NO_x) emissions by 12.91%. Furthermore, navigation speed optimization based on the refined propeller design yields a 3.05% reduction in the total fuel consumption and a 10.39% decrease in the total NO_x emissions when voyage time constraints are not considered, albeit with a 3.57% increase in total navigation duration. Under voyage time constraints, the total fuel consumption and the total NO_x emissions are reduced by 1.97% and 8.31%, respectively, while total navigation time decreases by 2.92%. These findings indicate that the proposed multi-objective optimization method based on NSGA-II and TOPSIS effectively enhances ship energy efficiency and environmental performance. By integrating operational and design parameter optimization while simultaneously addressing economic and ecological considerations, this study offers valuable insights for advancing ship energy efficiency strategies.

1. Introduction

Maritime transportation, characterized by its large carrying capacity and low unit transportation cost, plays a crucial role in global trade, accounts for approximately 80% of global trade volume and 70% of trade value [1]. However, this substantial cargo volumes transported via shipping—propelled predominantly by fossil fuels such as heavy fuel oil or marine diesel oil in conventional marine diesel engines— contribute significantly to atmospheric pollutants and greenhouse gas (GHG) emissions, presenting severe environmental challenges [2, 3]. In response, the International Maritime Organization (IMO) adopted a strategy in 2023 to

achieve net-zero GHG emissions by 2050, using 2008 levels as a baseline [4]. Additionally, regulatory measures such as the Energy Efficiency Design Index (EEDI) and the Ship Energy Efficiency Management Plan (SEEMP) have been implemented to enhance ship energy efficiency [5, 6]. Consequently, improving ship energy efficiency is not only essential for reducing shipping costs but also a critical requirement for compliance with IMO regulations [7,8].

Ship energy efficiency optimization is a multidimensional challenge encompassing operational optimization, technological advancements in equipment, crew awareness programs, shore-based collaborative support, design optimization, and trend analyses in energy efficiency [9]. The primary objective of these efforts is to minimize energy consumption and GHG emissions while maintaining operational efficiency [10]. In practical applications, optimization strategies must align with the vessel's operational purpose, route characteristics, and cost-benefit considerations [11].

Enhancing ship energy efficiency through propulsion system optimization has been extensively studied, with a particular focus on propeller performance improvements. As a key propulsion component, the optimization of propeller geometry and efficiency has attracted considerable research interest. Several studies [12-14] have employed optimization algorithms to refine propeller design, treating geometric parameters as optimization variables and propeller performance as the objective function. These approaches integrate geometric modelling and deformation techniques, iteratively generating optimized propeller designs that meet specified requirements. Mirjalili et al. [15] framed the propeller optimization problem with 20 design parameters and applied the Ant Lion Optimization (ALO) algorithm to derive optimal configurations. Tadros et al. [16] optimized the engine specific fuel oil consumption (SFOC) by incorporating cavitation performance constraints, achieving improved fuel efficiency rather than solely focusing on propeller efficiency. Esmailian et al. [17] introduced a lifecycle-based optimization framework using the Non-dominated Sorting Genetic Algorithm II (NSGA-II) to balance fuel consumption and cost.

To enhance the realism of optimization models, the effect of engine-propeller coupling has been considered in propeller optimization design. Taskar et al. [18] investigated the impact of engine-propeller matching on ship performance under varying sea conditions using coupled engine and propeller simulations. Similarly, Marques et al. [19] applied the differential evolution optimization algorithm to optimize engine-propeller matching in rough weather conditions. While existing research has made significant progress in improving propeller efficiency, fuel economy, and engine-propeller coupling considerations, limited attention has been given to multi-objective optimization approaches that simultaneously account for economic performance, emissions, and propulsion efficiency.

Another key strategy for enhancing ship energy efficiency is sailing speed optimization, which directly influences fuel consumption and emissions [20, 21]. Studies have demonstrated that reducing the sailing speed by 2–3 knots relative to the design speed can significantly decrease fuel consumption [22]. Sailing speed optimization typically relies on meteorological and sea condition forecast, operational task requirements, and cost assessments. Optimization algorithms are employed to determine the most economical speed profile, using sailing speed as the primary decision variable. Lu et al. [23] developed a multi-ship fuel consumption prediction model incorporating the effects of wind and waves, making the sailing speed optimization more practical for real-world applications. Given the dynamic nature of maritime navigation, Norstad et al. [24] applied dynamic optimization algorithms to optimize speed on tramp shipping routes, maximizing economic benefits. Bekir Sahin et al. [25] designed a multi-layer, multi-stage iterative optimization algorithm for dynamic route and path planning. Other studies have integrated propulsion system simulations into sailing speed optimization to further reduce fuel consumption and emissions.Theotokatos et al. [26] developed an integrated simulation model for commercial ship propulsion systems to optimize fuel consumption and carbon dioxide emissions. Fagerholt et al. [27] extended sailing speed optimization by incorporating emissions such as sulfur oxides and NO_x and considering emission control areas (ECAs) with sulfur emission limits. Yan et al. [28] used the K-means clustering algorithm to divide navigation segments based on marine environmental factors, establishing an energy efficiency optimization model and using particle swarm optimization (PSO) to refine main engine speed settings.

For real-time energy efficiency management, Wang et al. [29] employed a wavelet neural network to predict short-term operating conditions influenced by navigation environments, optimizing engine speeds through a real-time energy efficiency model. Zheng et al. [30] designed a data-driven ship energy efficiency management system capable of real-time monitoring of dynamic and static parameters, calculating EEDI and Energy Efficiency Operational Indicator (EEOI). While current research primarily focuses on optimizing sailing speed to reduce fuel consumption and pollutant emissions [31], relatively little attention has been given to the collaborative optimization of sailing speed and ship design parameters.

This study aims to propose a multi-objective optimization method for ship energy efficiency that accounts for actual sailing conditions, enabling the integrated optimization of propeller design parameters and sailing speed. To achieve this, a mathematical model of the ship-engine-propeller system is established, incorporating the effects of sea conditions. Based on this, the optimization models for propeller geometry and sailing speed are designed. Then, the NSGA-II is employed in conjunction with the Technique for Order of Preference by Similarity to Ideal Solution (TOPSIS) to determine optimal propeller parameters and navigation speeds for a given route. From a technical perspective, optimizing propeller design parameters enhances propulsion efficiency and minimizes energy consumption, while rational speed optimization prevents unnecessary fuel usage and emissions resulting from suboptimal navigation speeds. By integrating design and operational optimizations, this approach provides a comprehensive strategy for improving ship energy efficiency. Moreover, by effectively reducing greenhouse gas (GHG) emissions, this research contributes to the maritime industry's long-term sustainability goals, particularly the IMO's objective of achieving net-zero emissions by 2050.

The structure of this paper is as follows: Section 2 describes an overview of the proposed optimization method. Section 3 details the ship-engine-propeller system mathematical model, as well as the propeller and sailing speed optimization models. Then, Section 4 presents the parameters and data of the research subject. Next, Section 5 discusses the optimization results. Finally, Section 6 summarizes the conclusions and future research work.

2. Methodology

2.1 Overview of the Method

This paper proposes a multi-objective optimization method that comprehensively considers both ship operational optimization and design optimization. As shown in Figure 1, the method includes the following two optimization processes.

(a) Propeller Optimization

First, a mathematical model of the ship-engine-propeller system under different sea conditions is constructed based on ship and propeller parameters. Using propeller blade number, pitch ratio, disc area ratio, the propeller speed, and propeller diameter as optimization variables, a propeller optimization model is formulated. Then, a propeller optimization model is developed with the number of blades, pitch ratio, diameter ratio, the propeller speed, and propeller diameter as optimization variables. The model aims to minimize SFOC and nitrogen oxide (NO_x) emissions, while maximizing propulsive system efficiency through multi-objective optimization, resulting in the optimal propeller parameters.

(b) Sailing Speed Optimization

Based on the optimization results of the propeller, the sailing speed optimization model is constructed using sailing data, with the sailing speed of each segment of the sailing as the optimization variable. The model aims to minimize the total fuel consumption and NO_x emissions for the entire sailing through multi-objective optimization, yielding the optimal sailing speed for each segment to achieve ship energy efficiency optimization.

Both optimization processes are implemented on the MATLAB platform, using NSGA-II for iterative optimization, and TOPSIS is employed for performance ranking of the optimization results. The highest-rated solution is selected as the optimal solution.
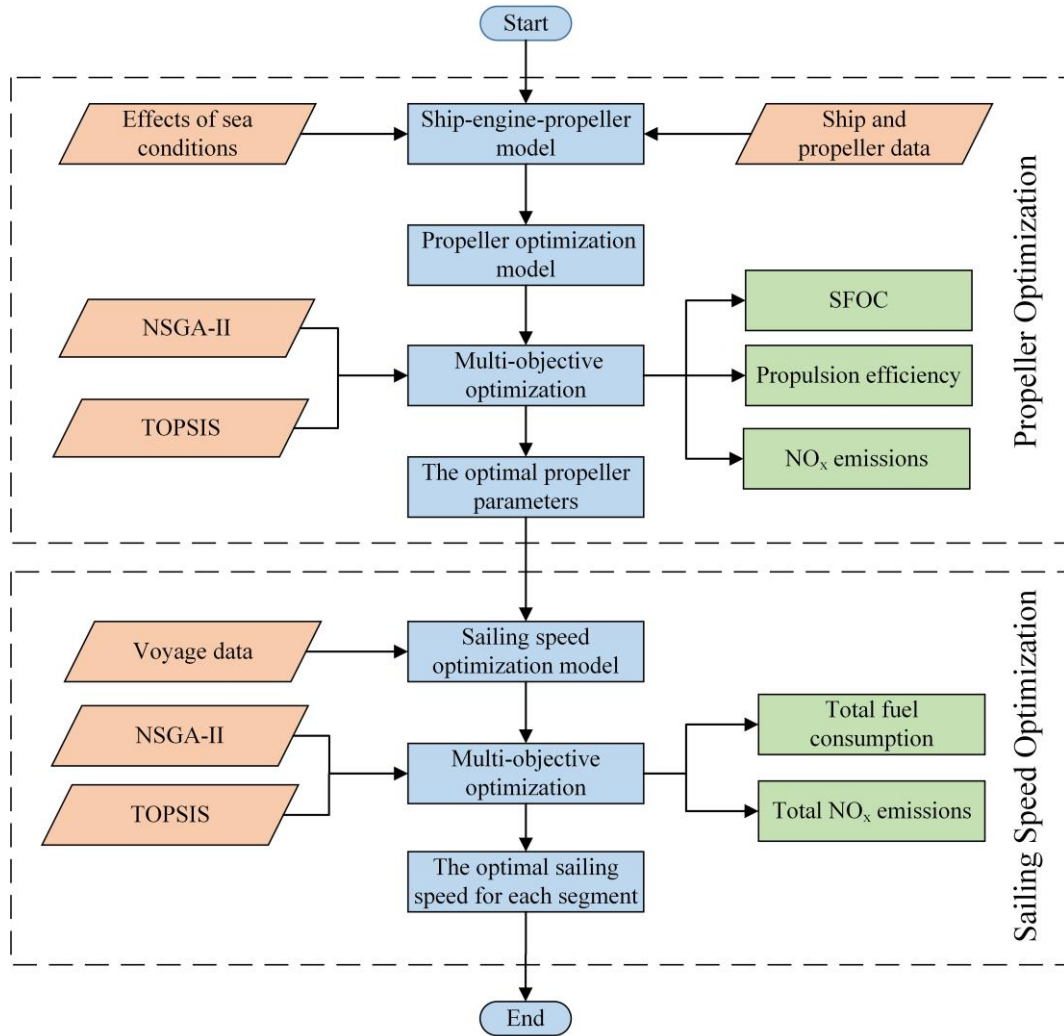
Fig. 1 Flowchart of ship energy efficiency multi-objective optimization method based on NSGA-II and TOPSIS

2.2 The Non-dominated Sorting Genetic Algorithm II (NSGA-II)

NSGA-II , a widely adopted multi-objective algorithm, is suitable for optimizing the three objectives of ship energy efficiency in this study: propulsion efficiency, emissions, and economy. This algorithm, proposed by Deb et al. [32], guarantees the even distribution of Pareto optimal solutions and has the advantages of fewer computational iterations and fast convergence [33]. In this study, the NSGA-II algorithm is used to solve the Pareto front of the objective function, and the solution process is shown in Figure 2 [34]:

Step 1: First, initialize and encode the optimization parameters that need to be optimized (such as the propeller pitch ratio P/D, disc area ratio A_E/A_0, the propeller speed n_p, propeller diameter D, number of blades Z, or the sailing speeds of each segment $v_1, v_2, \cdots, v_{19}$).

Step 2: Set the optimization range of parameters according to the range of optimization variables and constraints, and initialize the initial population.

Step 3: Perform non-dominated sorting and crowding distance calculation on the initialized population.

Step 4: Based on non-dominated sorting and crowding distance, select individuals for crossover and mutation operations to generate the next generation population.

Step 5: Perform non-dominated sorting and crowding distance calculation on the generated offspring population, and use an elitist strategy to update the population. These operations will continue until the specified number of iterations is reached.

Step 6: Finally, the Pareto front solutions for propeller optimization or each segment speed optimization can be obtained.
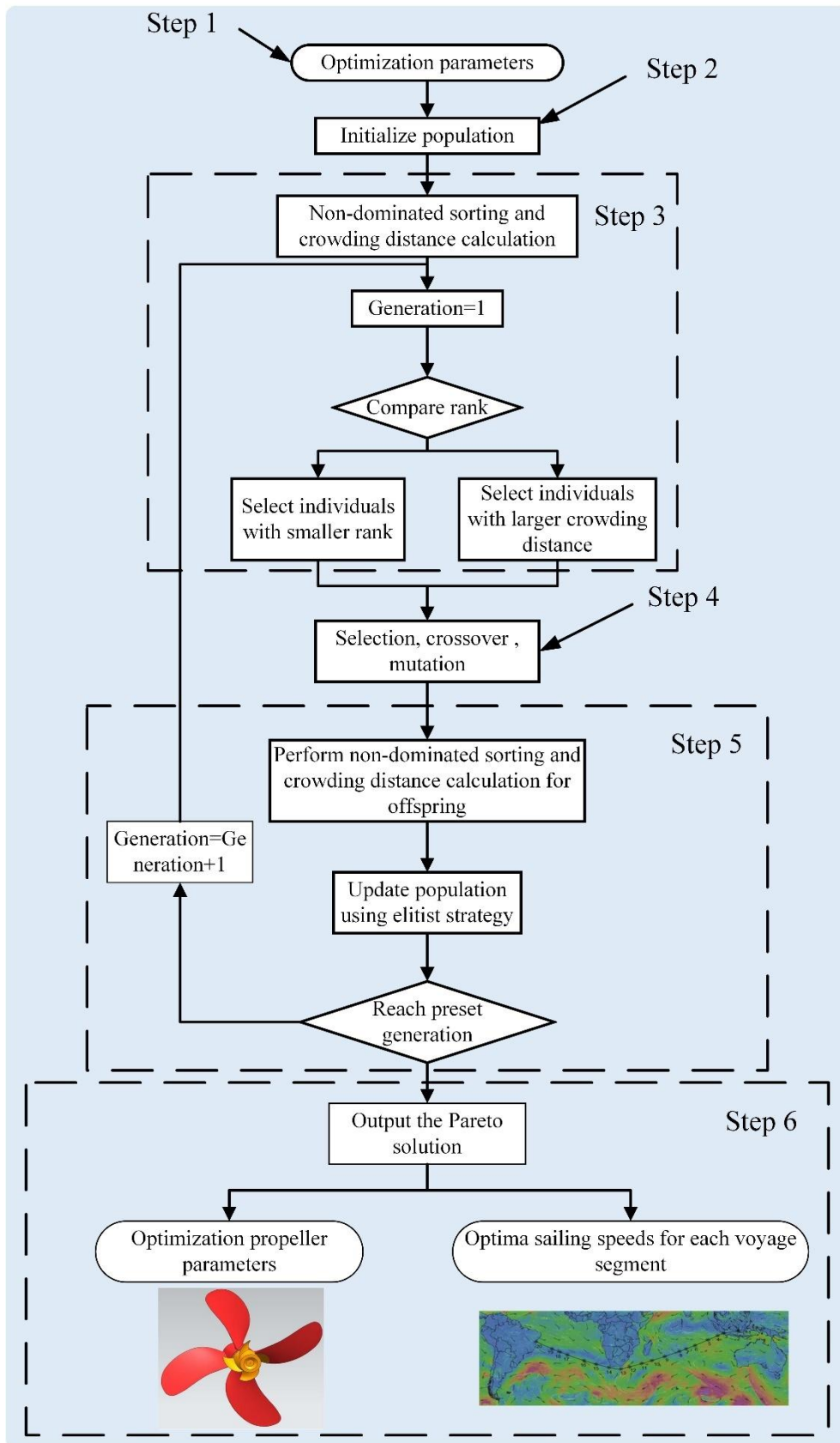
Fig. 2 Optimization process of the NSGA-II genetic algorithm

2.3 Technique for Order of Preference by Similarity to Ideal Solution (TOPSIS)

Due to the varying contributions among multiple optimization objectives in this study, it is necessary to scientifically evaluate and determine the weight of each objective by considering the influence factors.

TOPSIS, an efficient multi-criteria decision-making (MCDM) method , ranks alternative solutions by evaluating their proximity to the ideal solution, effectively addressing multi-objective decision-making problems [35]. In practical optimization design, only a few or even one optimal solution is often required. Therefore, the objective function is defined as the performance evaluation index, and the TOPSIS method is employed to perform multi-attribute decision-making on the Pareto solution set obtained from the NSGA-II algorithm [36]. To ensure objectivity and credibility of the evaluation results, the entropy weight method is applied to determine the weights of the indicators [37]. This method quantifies raw data disorder to objectively compute multidimensional indicator weights, eliminating subjective biases by leveraging inherent information entropy[38].

(1) Based on m candidate propeller designs or sailing speed optimization solutions and n evaluation criteria (propulsion efficiency $f(1)$,economic performance $f(2)$ and emissions $f(3)$ as detailed in Section3.2), construct the evaluation matrix $H = \left(h_{ij}\right)_{m \times n}$, where h_{ij} represents the j-th indicator value of the i-th candidate solution.

(2) Compute the proportion $p_{ij} = \frac{h_{ij}}{\sum_{i=1}^{m} h_{ij}}$ for each solution under each indicator, and then determine the information redundancy value $d_j = 1 + \frac{1}{\ln m} \sum_{i=1}^{n} p_{ij} \ln p_{ij}$.

(3) Compute the target weight $\omega_j = \frac{d_j}{\sum_{j=1}^{m} d_j}$ based on the entropy weight method through the obtained information redundancy value.

(4) Compute the normalized matrix $R = \left(r_{ij}\right)_{m \times n}$, as follows $r_{ij} = h_{ij} / \sqrt{\sum_{i=1}^{m} h_{ij}^2}$. Then, calculate the weighted normalized decision matrix $T = \left(t_{ij}\right)_{m \times n}$, where $t_{ij} = r_{ij} \cdot \omega_{ij}$, $i = 1,2,\cdots,m$, $j = 1,2,\cdots,n$.

(5) Identify the ideal solution H_i^+ and the anti-ideal solution H_i^- for each evaluation criterion i, d_i^+, d_i^-:

$$d_i^+ = \sqrt{\sum_{j=1}^{n} \left(t_j^+ - t_{ij}\right)^2} \tag{1}$$

$$H_i^+ = \left\{\left(\max_i t_{ij} \middle| j \in J^+\right), \left(\min_i t_{ij} \middle| j \in J^-\right)\right\} = \left\{t_j^+ \middle| j = 1,2,\cdots,n\right\} \tag{2}$$

$$d_i^- = \sqrt{\sum_{j=1}^{n} \left(t_j^- - t_{ij}\right)^2} \tag{3}$$

$$H_i^- = \left\{\left(\min_i t_{ij} \middle| j \in J^+\right), \left(\max_i t_{ij} \middle| j \in J^-\right)\right\} = \left\{t_j^- \middle| j = 1,2,\cdots,n\right\} \tag{4}$$

where, $J^+ = \{j = 1,2,\cdots,n|j\}$ represents the set of beneficial indicators, while $J^- = \{j = 1,2,\cdots,n|j\}$ represents the set of non-beneficial indicators.

(6) Compute the relative closeness E_i^* of each candidate solution to the ideal solution using:

$$E_i^* = J_i^- / (J_i^- + J_i^+), 0 \leq E_i^* \leq 1 \tag{5}$$

(7) Rank all candidate solutions based on E_i^*, and select the solution with the highest score as the optimal propeller design or sailing speed solution.

3. Model Description

3.1 Ship-Engine-Propeller Model

3.1.1 Ship Resistance

For large ships, the energy consumed to overcome resistance constitutes the majority of the input energy. Ship resistance includes basic resistance and added resistance. Basic resistance R_T refers to the resistance encountered by the hull moving in calm water, while added resistance accounts for external factors such as wind, waves, and currents [39]. Therefore, the total resistance R_{total} can be expressed as follows:

$$R_{total} = R_T + R_{wind} + R_{wave} \tag{6}$$

(1) The resistance in calm water R_T

R_T is divided into six components [40]: viscous resistance of the bare hull R_F, wave-making resistance R_W, transom stern immersion resistance R_{TR}, additional bulbous bow resistance R_B, appendage resistance R_{APP}, and the model-ship correlation resistance R_A:

$$R_T = R_F + R_{APP} + R_W + R_B + R_{TR} + R_A \tag{7}$$

(2) The added wind resistance R_{wind}

R_{wind} is calculated as [41]:

$$R_{wind} = 0.5X'_W(\varepsilon)\rho_a V_{wr}^2 A_F \tag{8}$$

where, ρ_a is the air density, A_F is maximum transverse area of the hull above the water surface, $X'_W(\varepsilon)$ is the non-dimensional aerodynamic drag coefficient, and V_{wr} is the relative wind speed.

(3) The added wave resistance R_{wave}

R_{wave} is defined by referring to the semi-empirical prediction formula based on Gerritsma and Beukelman's method [23, 42]:

$$R_{wave} = \frac{-k\cos\beta^2}{2\omega_e}\int_0^L b'\left|V_{Z_b}\right|^2 \mathrm{d}x_b \tag{9}$$

where, k is wave number, β is heading angle, ω_e is frequency of encounter, L is ship's water line length, V_{Z_b} is the amplitude of the velocity of water relative to the strip, b' is the sectional damping coefficient for speed, x_b is x coordinate on the ship.

(4) The effects of ocean currents

To account for the effects of ocean currents, this study applies a current disturbance modeling method based on velocity vector synthesis. This method simplifies the ocean current into uniform flow and represents its influence on ship motion as the variation between relative velocity and displacement of the current:

$$u_C = V_s + V_c\cos(\Psi_c - \Psi) \tag{10}$$

where V_c is the current velocity, V_s is sailing speed, Ψ_c is the current direction, and u_C is the advance velocity component.

3.1.2 Propeller Torque and Effective Thrust

To overcome the resistance during navigation, the main engine drives the propeller via a transmission shaft, providing thrust to propel the ship. The propeller's effective thrust T_e and torque Q are given as [43]:

$$T_e = (1-t)K_T\rho n_p^2 D^4 \tag{11}$$

$$Q = K_Q\rho n_p^2 D^5 \tag{12}$$

where, t is the thrust deduction coefficient, ρ is the seawater density, D is the propeller diameter, n_p is the revolutions per minute (RPM) of the propeller, K_T and K_Q are the thrust and torque coefficients of the propeller. These coefficients are obtained from the B-series propeller charts developed by the Netherlands Ship Model Basin [44]:

$$K_T = \sum_{n=1}^{39} C_n \, (P/D)^{t_n} (J)^{s_n} (A_E/A_0)^{u_n} (Z)^{v_n} \tag{13}$$

$$K_Q = \sum_{n=1}^{47} C_n \, (P/D)^{t_n} (J)^{s_n} (A_E/A_0)^{u_n} (Z)^{v_n} \tag{14}$$

where P/D is the propeller pitch ratio, A_E/A_0 is the propeller area ratio, Z is the number of blades, C_n, t_n, s_n, u_n, v_n are regression coefficients, and J is the advance coefficient defined as [45]:

$$J = V_s(1 - \omega)/(n_p D) \tag{15}$$

where w is the wake fraction. The calculation methods of the propeller thrust deduction coefficient t and the wake fraction coefficient ω under different working conditions are as follows:

$$t = \begin{cases} 0.33, & n < -n_e \\ -0.33\dfrac{n}{n_e}, & -n_e < n < 0 \\ t_0\dfrac{n}{n_e}, & 0 \le n < n_e \\ t_0, & n \ge n_e \end{cases} \tag{16}$$

$$\omega = \begin{cases} 0, & V_S \le 0 \\ \omega_0 \dfrac{V_S}{V_{se}}, & 0 < V_S < V_{se} \\ \omega_0, & V_S > V_{se} \end{cases} \tag{17}$$

where, t_0 represents the thrust deduction of the ship's propeller at the rated rotational speed; n_e represents the rated rotational speed of the ship's propeller; V_{se} represents the rated speed of the ship; and ω_0 represents the wake fraction coefficient of the ship at the rated speed.

3.1.3 Main Engine Fuel Consumption

Main engine fuel consumption is a critical factor in sailing costs. The fuel oil consumption FOC is calculated as [46]:

$$FOC = SFOC \cdot P_b \cdot T \tag{18}$$

where, $SFOC$ is the specific fuel oil consumption of the engine, T is the sailing time, and P_b is the engine brake power given by:

$$P_b = K_Q \rho D^5 n_e^3/(9550\eta_t) \tag{19}$$

where, n_e is the engine speed, η_t is transmission efficiency.

3.1.4 Sailing Speed

When a ship is sailing steadily under specific conditions, the engine speed n_p is approximately linearly related to the sailing speed V_s:

$$n_p = aV_s + b \tag{20}$$

where a and b are fitting coefficients. For ships using direct propulsion, the engine speed n_e equals the propeller speed n_p. Thus, the fuel consumption can be expressed as a function of sailing speed by combining Eq. (16)-(18).

3.1.5   Model Validation

Figure 3 compares the experimental and calculated torque values under 19 engine load conditions (between 20% and 110% loads, every 5% of the load was taken as an operating point). The results show that the calculated torque values closely match the experimental data, with a percentage deviation of less than 1% across all load levels. This confirms that the developed ship-engine-propeller model achieves sufficient simulation accuracy and is suitable for energy efficiency optimization studies in this research.
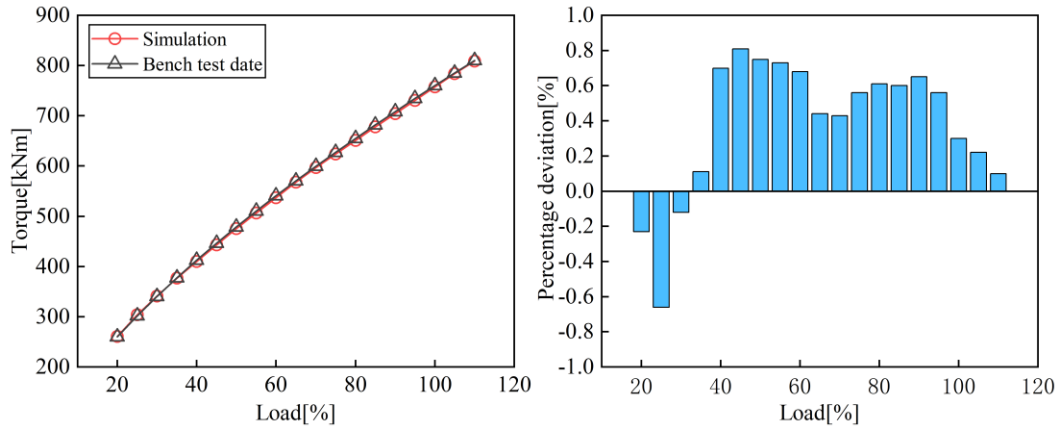
Fig. 3 Model verification under different loads

3.2 Propeller Optimization Model

Based on the ship-engine-propeller mathematical model, a multi-objective optimization model for the propeller is constructed with the objectives of maximizing propulsion efficiency, minimizing SFOC, and reducing NO_x emissions:

$$minf(X_1) = [1/f(1), f(2), f(3)] \tag{21}$$

$$\text{s.t.} \begin{cases} D_{min} \le D \le D_{max} \\ (n_p)_{min} \le n_p \le (n_p)_{max} \\ (P/D)_{min} \le (P/D) \le (P/D)_{max} \\ (A_E/A_0)_{min} \le (A_E/A_0) \le (A_E/A_0)_{max} \\ Z_{min} \le Z \le Z_{max} \\ T(1-t) = R \\ P_s \eta_s \eta_R = 2\pi n Q \\ A_E/A_0 \ge (1.3 + 0.3Z)T/(P_0 - P_V) + K \end{cases} \tag{22}$$

The optimization variables $X_1 = [D, n_p, P/D, A_E/A_0, Z]$ and their respective ranges are shown in Table 1.

Table 1 Propeller optimization variables

Parameter	Symbol	Range	Unit
Propeller diameter	D	6.5—8.5	m
RPM of propeller	n_p	50—83	rpm
Pitch ratio	P/D	0.5—1.4	—
Expanded area ratio	A_E/A_0	0.3—1.05	—
Number of blades	Z	2—7	—

The objective function $f(1)$ represents the propulsion efficiency η, expressed as:

$$\eta = \eta_H \cdot \eta_0 \cdot \eta_R \cdot \eta_S \tag{23}$$

where, hull efficiency η_H, scale effect efficiency η_S and relative rotation efficiency η_R are constants. η_0 is open water efficiency of the propeller. Thus, the objective function is simplified to [47]:

$$f(1) = \eta_0 = (J \cdot K_T)/(2\pi \cdot K_Q) \tag{24}$$

The objective functions $f(2)$ and $f(3)$, represent the main engine's $SFOC$ and NO_x emission rate (E_{NO_x}). Polynomial fitting of the engine's $SFOC$ and NO_x emission rate E_{NO_x} curves using MATLAB yields functions dependent on the propeller speed n_p:

$$f(2) = -3.56 * 10^{-6} * n_p^5 + 1.19 * 10^{-3} * n_p^4 - 0.16 * n_p^3 + 1.02 * n_p^2 - 327.34 \\ * n_p + 4335 \tag{25}$$

$$f(3) = -3.95 * 10^{-4} * n_p^3 + 0.07 * n_p^2 - 4.35 * n_p + 103.71 \tag{26}$$

Two constraints are established based on the kinematic relationship of the propulsion system (balancing propeller thrust with ship resistance) and energy conservation (balancing propeller load with diesel engine output power):

$$T(1 - t) = R_{total} \tag{27}$$

$$P_s \eta_s \eta_R = 2\pi n_p Q \tag{28}$$

To ensure the designed propeller's disc area ratio meets cavitation check requirements, an additional constraint is added:

$$A_E/A_0 \geq (1.3 + 0.3Z)T/(P_0 - P_V) + K \tag{29}$$

where P_0 is the static pressure at the propeller shaft centre, P_V is the vapour pressure of water, and K is a coefficient (0.2 for single-screw vessels).

3.3 Sailing Speed Optimization Model

Based on the ship-engine-propeller mathematical model and the optimized structural propeller parameters, a sailing speed optimization model is developed. The total fuel consumption and total NO_x emissions over the sailing are considered as optimization objectives:

$$minf(X_2) = [f(4), f(5)] \tag{30}$$

$$s.t. \begin{cases} v_{min} \leq v_i \leq v_{max} \\ \sum S_i = S_0 \end{cases} \tag{31}$$

The optimization variable X_2 represents the sailing speed for each sailing segment:

$$X_2 = [v_1, v_2, \cdots, v_{19}] \tag{32}$$

The objective functions $f(4)$ and $f(5)$ are defined as the total fuel consumption and total NO_x emissions:

$$f(4) = FOC_{total} = \sum_{i=1}^{n}(SFOC_i \cdot P_i \cdot T_i) \tag{33}$$

$$f(5) = \sum_{i=1}^{n}(P_i \cdot E_{NO_{X_i}} \cdot T_i) \tag{34}$$

where FOC_{total} is the total fuel consumption for the sailing; $SFOC_i$ is the specific fuel oil consumption rate for each segment; T_i is the sailing time for segment; $E_{NO_{x}i}$ is the NO_x emission rate for segment.

To ensure the consistency of the sailing path, a constraint is set to maintain the total sailing distance S_0 unchanged before and after optimization:

$$\sum S_i = S_0 \tag{35}$$

In order not to increase the total sailing time of the voyage, the total sailing time can be set as a constraint condition, that is, the optimized total sailing time should not exceed the original total sailing time:

$$\sum t_i \leq t_0 \tag{36}$$

4. Research Object and Data

The research object of this study is a 49,900 DWT oil tanker Stena Prosperous, equipped with a MAN 6G50ME two-stroke low-speed engine. The main technical specifications of the ship and engine are provided in Tables 2 and 3.

Table 2 Main Technical Parameters of the Ship

Parameter	Symbol	Value	Unit
Length between perpendiculars	L_{PP}	186	m
Breadth	B	32.2	m
Depth	D	18.35	m
Design draft	d	11.5	m
Gross tonnage	W	29884	t

Table 3 Main Technical Parameters of the Engine

Parameter	Value	Unit
Number of cylinders	6	-
Cylinder bore	500	mm
Piston stroke	2500	mm
Rated power	6400	kW
Rated speed	80.4	rpm
SFOC	167.36	g/kWh

The studied route spans from the IDTRH port in Indonesia to the BRARB port in Brazil, with a total sailing distance of 9,614.24 nautical miles and a sailing time of 782.01 hours. The monthly average wind speed topology for June 2024 corresponding to this route is shown in Figure 4.

The route is divided into 19 segments (as shown in Figure 5) based on the following principles:

(a) The ship's course remains relatively constant within each segment;

(b) The hydrological and meteorological conditions are similar.

Within each segment, it is assumed that the ship travels at a constant speed, and the engine speed remains constant.

Based on the above principles and assumptions, the detailed data for each route segment were determined, as shown in Table 4. The parameters include sailing distance, sailing time, Beaufort number (BN), average encounter angle θ_l, the sailing speed for each sailing segment v_i, the engine speed, SFOC, NO_x emission rate.
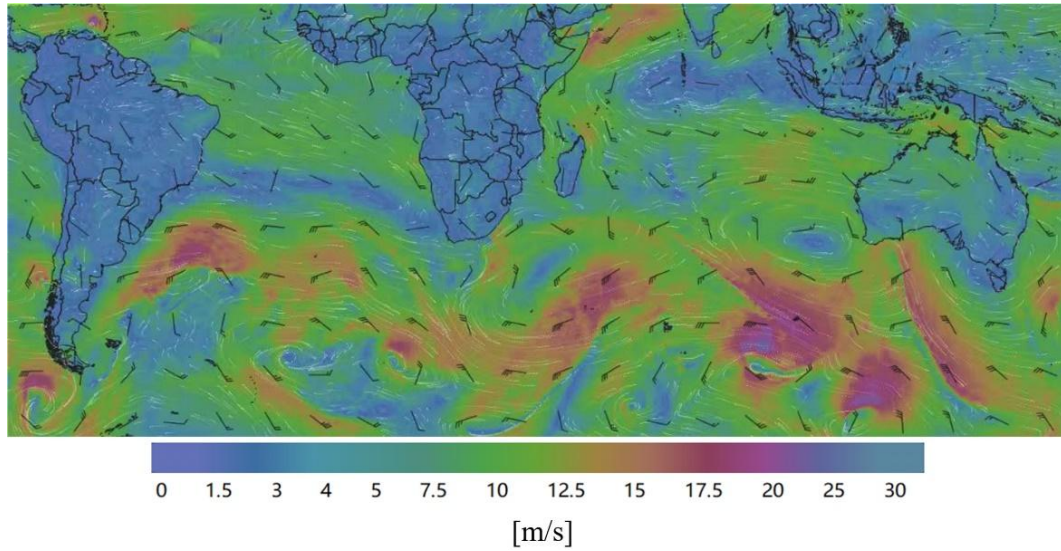
Fig. 4 Topology of absolute wind speed in June 2024

Table 4 Voyage data

segment	S_i [n mile]	T [h]	BN	θ_l[°]	v_i[kn]	$SFOC$ [g/kWh]	E_{NO_x} [g/kWh]	n_e[rpm]
1-2	82.29	6.81	4	35.7	12.1	155.3	10.64	68.9
2-3	713.18	51.09	3	167.7	14.1	156.0	6.68	79.8
3-4	301.73	25.15	5	138.2	12	155.6	10.75	68.3
4-5	466.31	39.59	6	147.1	11.5	156.3	10.95	67.0
5-6	630.89	52.49	4	141.5	12.1	155.5	10.73	68.4
6-7	427.91	34.91	4	148.1	12.3	154.9	10.47	69.8
7-8	304.52	25.21	4	6.1	12.1	155.4	10.67	68.8
8-9	707.69	57.26	3	112.2	12.3	154.5	10.34	70.4
9-10	603.46	48.05	4	161.4	12.6	154.2	10.07	71.6
10-11	488.25	42.11	5	145.2	11.6	156.8	11.09	65.9
11-12	548.6	44.18	3	105.1	12.3	154.5	10.28	70.8
12-13	378.53	28.91	5	29.1	12.4	153.8	9.10	74.8
13-14	559.57	45.79	5	21.1	13.2	155.0	10.51	69.6
14-15	576.03	47.18	4	23.5	12.3	155.0	10.52	69.5
15-16	554.08	46.61	5	26.3	12.5	155.9	10.85	67.7
16-17	773.52	61.69	4	26.3	12.7	154.3	10.10	71.5
17-18	356.59	28.76	2	154.1	12.3	154.6	10.29	70.7
18-19	373.05	30.29	3	135.4	12.4	154.7	10.39	70.2
19-20	768.04	65.93	5	155.9	12.6	156.7	11.05	66.2
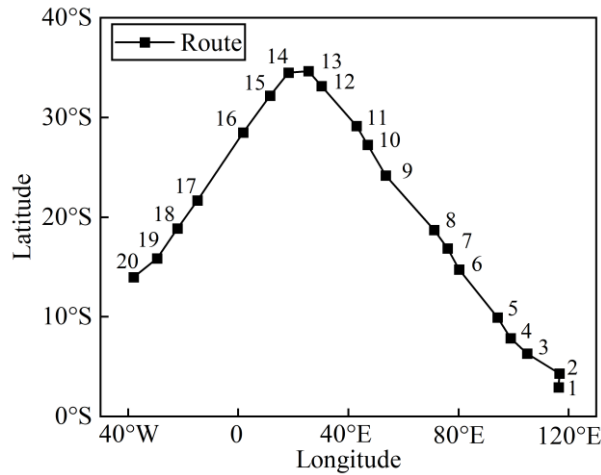
Fig. 5 The results of segment division from IDTRH Port to BRARB Port

5. Results and Discussion

5.1 Propeller Optimization

The optimization variables include the propeller pitch ratio, the blade area ratio, the propeller speed, diameter, and the number of blades. The optimization objectives are the propulsion efficiency, SFOC, and the specific NO_x emissions. The NSGA-II algorithm and TOPSIS comprehensive evaluation method were used to optimize the model. The NSGA-II parameter settings are provided in Table 5.

Table 5 The main parameters of NSGA-II

Parameter	Setting
population size	200
the number of generations	500
crossover probability	0.8

In view of the interrelation among the optimization objectives, when applying the decision-making theory based on TOPSIS, it is necessary to balance the weights of the three objectives of propulsion efficiency, SFOC, and the specific NO_x emissions to determine a set of optimal compromise solutions. The weights of each optimization objective are obtained by means of the entropy weight method: the propulsion efficiency is 0.18, SFOC is 0.37, and the specific NO_x emissions is 0.45. Among them, the weight of the specific NO_x emissions is the largest, which highly conforms to the concept of green shipping and can minimize environmental pollution. The weight of SFOC ranks second. Since it is not only related to energy utilization but also closely connected with carbon emissions, this weight setting takes into account both the operation cost and energy efficiency while ensuring environmental protection.

Firstly, the Pareto front solutions were obtained by using the NSGA-II optimization algorithm, as shown in Figure 6. Then, the TOPSIS method was used to conduct multi-attribute decision-making on the Pareto front solutions, and the results of the optimal solution were also marked in Figure 6.
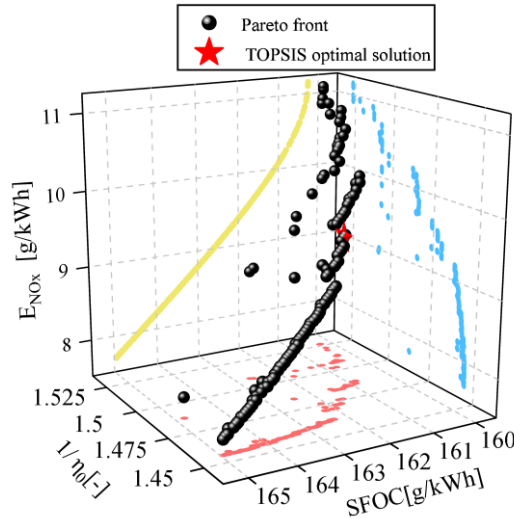
Fig. 6 Pareto chart of propeller optimization results

The comparison of the original and optimized results is presented in Table 6. The results indicate that the optimal parameters exhibit minor deviations from the original ones; however, significant improvements were achieved in terms of propulsive efficiency, fuel economy, and emission reduction. The optimized propulsion system demonstrates higher efficiency, reduced fuel consumption, and lower NO_x emissions. Specifically, propulsive efficiency increased by 2.11%, fuel consumption decreased by 1.93%, and NO_x emissions reduced by 12.91%.

Table 6 Comparison of original and optimization propeller parameters

Parameter	Original Value	Optimized Value	Improvement
$D[m]$	7.1	6.54	-
P/D	0.836	0.861	-
A_E/A_0	0.4	0.531	-
Z	4	4	-
n	69.9	75.1	-
η_0	0.661	0.675	2.11%
$SFOC[g/kWh]$	164.3	161.2	1.93%
$E_{NO_x}[g/kWh]$	11.42	9.95	12.91%

To further analyze the performance of the optimized propeller, the open water efficiency and thrust coefficient were calculated for both the original and optimized propellers. The results are illustrated in Figure 7. It is observed that the optimized propeller's thrust coefficient improved by 13.9%, 10.7%, and 6.6% at advance coefficients $J = 0.2$, $J = 0.4$, and $J = 0.6$, respectively, showing consistent superiority over the original propeller across all advance coefficients. Meanwhile, the open water efficiency of the optimized propeller increased by 5.7%, 3.5%, and 0.5% at $J = 0.2$, $J = 0.4$, and $J = 0.6$, respectively, achieving noticeable improvements under all operating conditions.
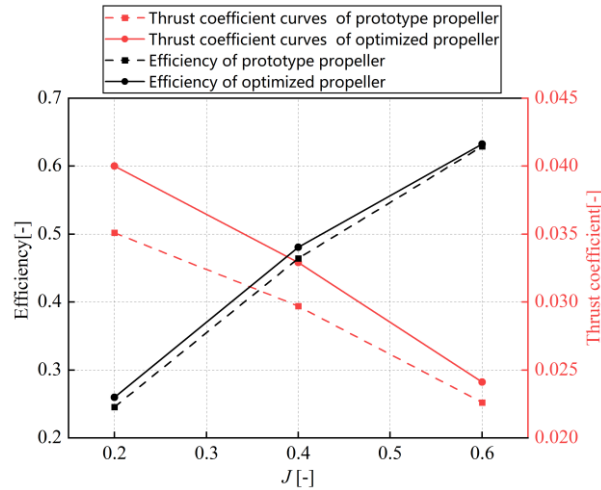
Fig. 7 Efficiency and thrust coefficient curves of optimized propeller and prototype propeller

5.2 Sailing Speed Optimization

The optimization model aims to determine the optimal sailing speed for each segment, using the NSGA-II and the TOPSIS method. Two optimization schemes were designed according to whether the sailing time is considered as a constraint condition. The NSGA-II parameter settings are provided in Table 7.

Table 7 The main parameters of NSGA-II

Parameter	Setting
population size	50
the number of generations	200
crossover probability	0.8
mutation probability	0.05

Since there is a certain correlation and mutual influence among the optimization objectives, when applying the decision-making theory based on TOPSIS, it is necessary to comprehensively consider the weights of these two optimization objectives, so as to select a set of optimal solutions as a compromise plan. The weights of the optimization objectives are determined by the entropy weight method: the weight of the total NO_x emissions is 0.54; the weight of the total fuel consumption is 0.46. The relatively high weight of the total NO_x emissions highlights the current emphasis on environmental protection. When screening the schemes, options that can significantly reduce NO_x emissions will be given priority, which helps to promote environmentally friendly development. The total fuel consumption is directly related to the operation cost of the ship, which is a factor that shipowners pay great attention to. Therefore, its weight is only slightly lower than that of the total NO_x emissions. In short, the setting of the weights of the optimization objectives ensures that while pursuing environmental benefits, economic costs and the efficient use of energy are also taken into account.

When the total sailing time is not considered as an optimization constraint, the Pareto front solutions are shown in Figure 8. Then, the TOPSIS method is used to conduct multi-attribute decision-making on the Pareto front solutions calculated by the NSGA-II algorithm, and the results of the optimal solution are also marked in Figure 8.
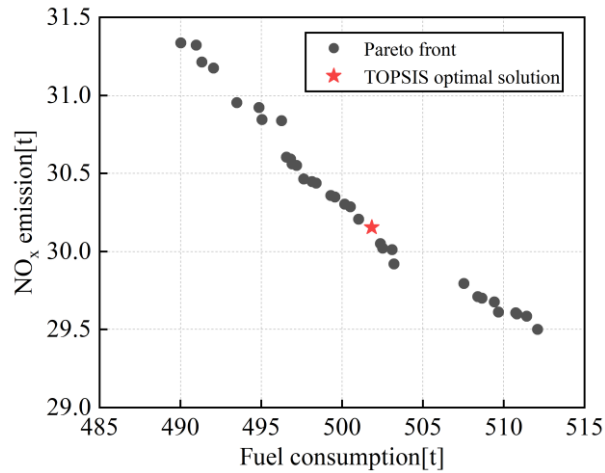
Fig. 8 Pareto chart of sailing speed optimization results without considering total sailing time as a constraint

The optimized results for each sailing segment are presented in Table 8, and the comparison with the original values is shown in Table 9. The results indicate that the fuel consumption was reduced from 517.6 t to 501.8 t, representing a 3.05% reduction, while the NO_x emissions decreased from 33.7 t to 30.2 t, achieving a reduction of 10.39%. Although the total sailing time increased from 782.01 h to 809.9 h (a 3.57% increase), the optimization significantly reduced fuel costs and emissions.

Table 8 Optimization results of each segment without considering total sailing time as a constraint

Segment	v_i [kn]	T [h]	n_p [rpm]	FOC [t]	NOx Emission [t]
1-2	10.61	7.74	60.18	3.29	0.23
2-3	12.02	59.31	68.44	36.14	2.50
3-4	13.81	21.84	78.94	20.40	0.94
4-5	11.08	42.05	62.93	20.30	1.46
5-6	9.78	64.47	55.28	21.67	1.63
6-7	9.82	43.55	55.51	14.81	1.11
7-8	13.62	22.35	77.84	19.92	1.01
8-9	10.21	69.28	57.80	26.37	1.95
9-10	10.84	55.64	61.51	25.20	1.83
10-11	10.45	46.68	59.23	19.02	1.39
11-12	13.72	39.96	78.44	36.54	1.76
12-13	11.69	32.375	66.48	18.20	1.28
13-14	11.39	49.08	64.76	25.66	1.83
14-15	13.96	41.25	79.84	40.03	1.71
15-16	13.77	40.22	78.73	37.23	1.75
16-17	12.20	63.35	69.52	40.34	2.75
17-18	13.97	25.51	79.92	24.85	1.05
18-19	13.20	28.26	75.35	22.73	1.31
19-20	13.47	56.98	76.99	49.02	2.61

The comparison of sailing speed, fuel consumption, and NO_x emissions in each voyage segment before and after optimization is shown in Figure 9. Through the optimization of the ship speeds in each voyage segment, fuel consumption and NO_x emissions have been significantly reduced, and the economic and environmental performance of the ship has been enhanced.

Table 9 Comparison of results before and after speed optimization without considering total sailing time as a constraint

Parameter	Original Value	Optimized Value	Improvement
Total Fuel Consumption [t]	517.6	501.8	3.05%
Total NO$_x$ Emissions [t]	33.7	30.2	10.39%
Sailing Time [h]	782.01	809.90	-3.57%
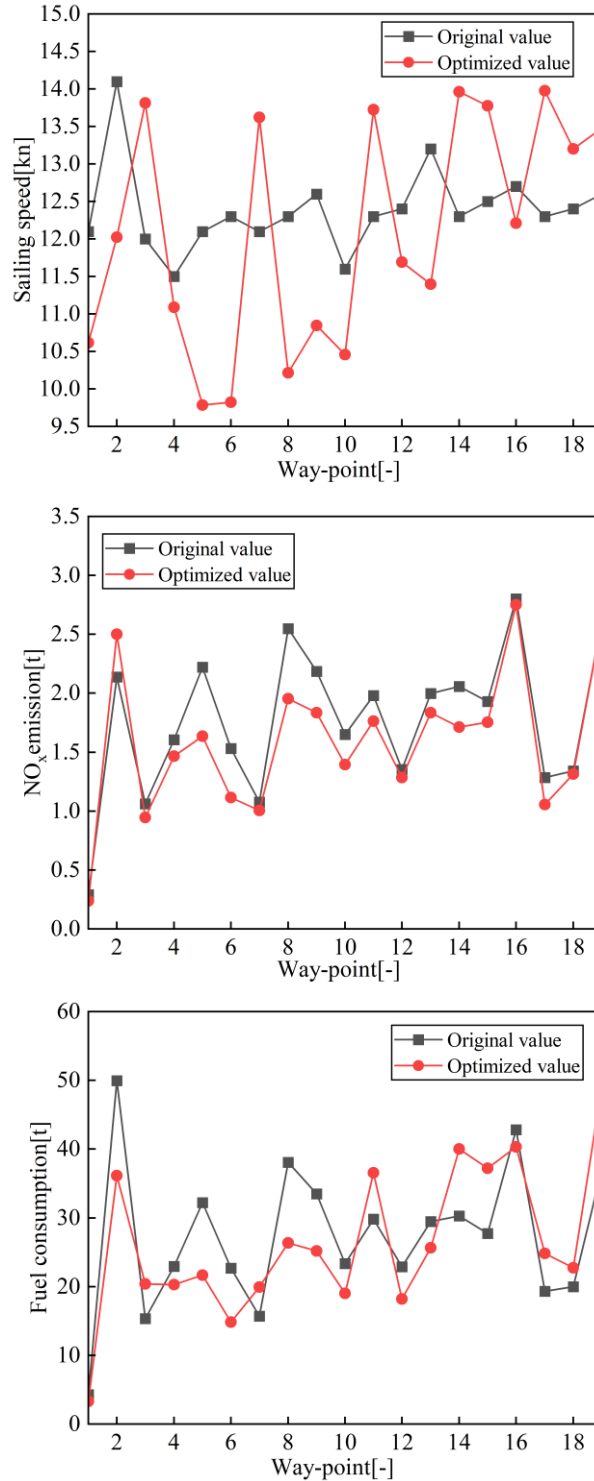
Fig. 9 Comparison of results before and after optimization without considering total sailing time as a constraint

17

When the total sailing time is considered as an optimization constraint, the Pareto front solutions are shown in Figure 10. Then, the TOPSIS method is used to conduct multi-attribute decision-making on the Pareto front solutions calculated by the NSGA-II algorithm, and the results of the optimal solution are also marked in Figure 10.
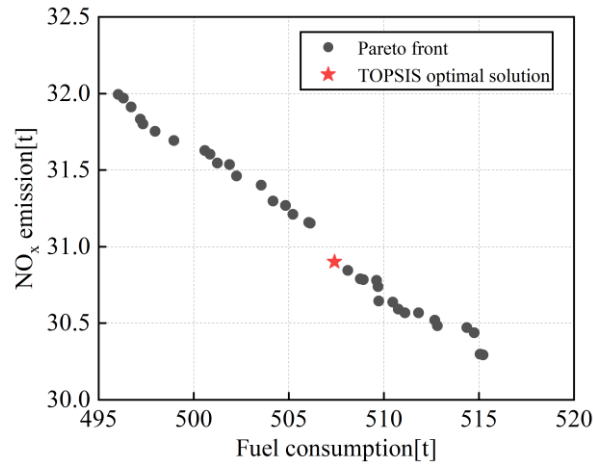
Fig. 10 Pareto chart of voyage speed optimization results considering total sailing time as a constraint

The optimized results of each voyage segment are shown in Table 10, and the comparison with the original data is shown in Table 11. The results show that after optimization, the fuel consumption has decreased from 517.6 tons to 507.4 tons, a reduction of 1.97%; the NO_x emissions have decreased from 33.7 tons to 30.9 tons, a reduction of 8.31%; and the total sailing time has decreased from 782.01 hours to 759.17 hours, a reduction of 2.92%. This optimization scheme has simultaneously optimized the fuel consumption, NO_x emissions, and sailing time.

Table 10 Optimization results of each segment considering total sailing time as a constraint

Segment	v_i [kn]	T [h]	n_p [rpm]	FOC [t]	NO_x Emission [t]
1-2	13.13	6.26	74.95	4.53	0.28
2-3	13.32	53.52	76.08	40.57	2.39
3-4	12.54	24.05	71.50	15.16	1.04
4-5	13.56	34.37	77.50	27.63	1.50
5-6	11.61	54.31	66.03	27.41	2.04
6-7	9.98	42.86	56.43	13.96	1.10
7-8	11.96	25.46	68.06	13.97	1.02
8-9	13.32	53.09	76.11	40.29	2.37
9-10	13.92	43.33	79.61	38.10	1.75
10-11	12.27	39.79	69.88	23.51	1.67
11-12	13.88	39.51	79.37	34.37	1.62
12-13	12.14	31.17	69.12	17.86	1.29
13-14	11.27	49.62	64.05	23.01	1.74
14-15	13.73	41.93	78.50	35.16	1.78
15-16	12.52	44.24	71.36	27.74	1.92
16-17	13.73	56.31	78.50	47.21	2.39
17-18	12.04	29.59	68.58	16.59	1.20
18-19	13.92	26.78	79.62	23.55	1.08
19-20	12.21	62.88	69.55	36.66	2.63

Table 11 Comparison of results before and after speed optimization considering total sailing time as a constraint

Parameter	Original Value	Optimized Value	Improvement
Total Fuel Consumption [t]	517.6	507.4	1.97%
Total NO$_x$ Emissions [t]	33.7	30.9	8.31%
Sailing Time [h]	782.01	759.17	2.92%
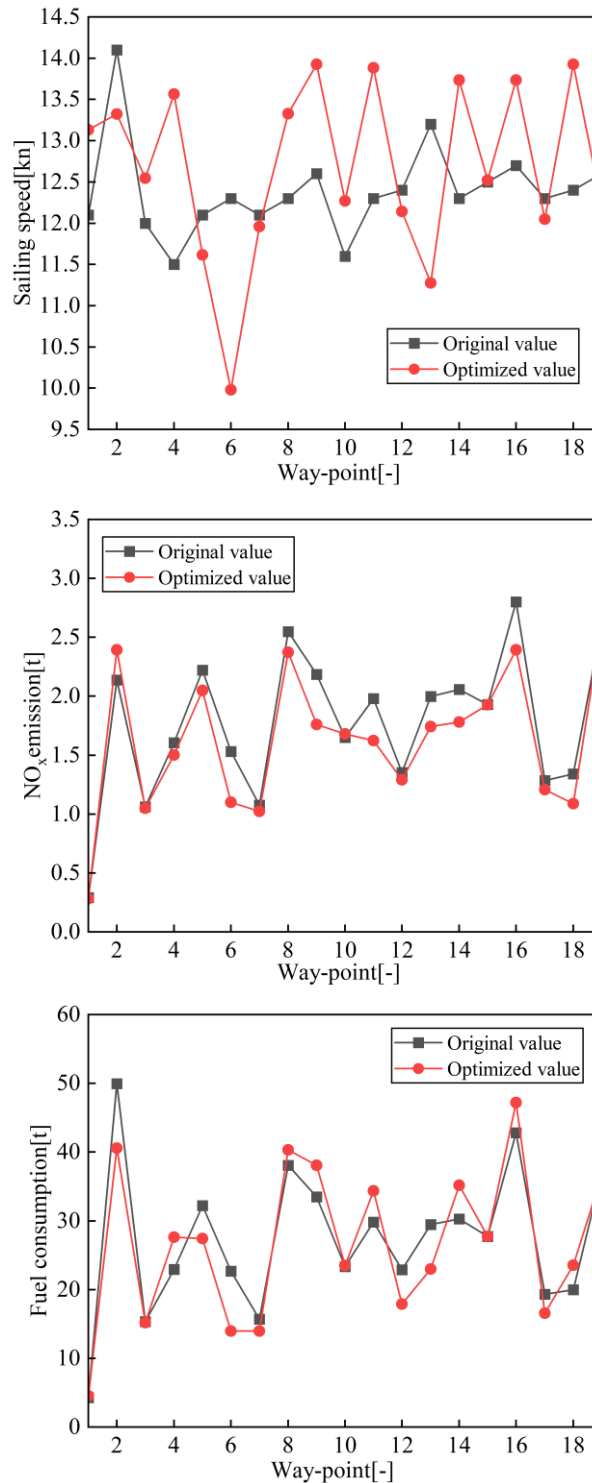
Fig. 11 Comparison of results before and after optimization considering total sailing time as a constraint

The comparison of the ship speeds, fuel consumption, and NO_x emissions in each voyage segment before and after optimization is shown in Figure 11. It can be seen that the average optimized ship speed is slightly higher than the original ship speed, which shortens the sailing time. A more scientific ship speed distribution is achieved through optimization.

A comprehensive comparison of the two ship speed optimization schemes shows that each has its own advantages and disadvantages. When the sailing time constraint is not considered, the reduction in fuel consumption and emissions is greater, but the voyage duration increases. Conversely, when voyage time is included as an optimization constraint, it can achieve reductions in fuel consumption and emissions while also shortening the voyage duration. Shipowners can choose between these two optimization schemes based on the correlation between voyage time and commercial interests.

6. Conclusion

This study comprehensively considers the optimization of both operational and design parameters for ships and proposes a multi-objective optimization method for ship energy efficiency based on the NSGA-II algorithm and the TOPSIS approach. The proposed method aims to improve ship navigation efficiency while reducing fuel consumption and NO_x emissions.

This method was applied to optimize the structural parameters of the propeller for a 49,900 DWT oil tanker. The optimization results showed a 2.11% improvement in propeller propulsion efficiency, a 1.93% reduction in fuel consumption rate, and a 12.91% decrease in NO_x emission rate. This method can be applied not only to the maintenance (propeller replacement) of existing ships but also to the design of new ships.

Based on the optimized propeller parameters, two schemes were designed to optimize the sailing speed for the same target vessel over a single sailing. When the sailing time constraint is not considered, the optimization results show that with a 3.57% increase in the total sailing time, the total fuel consumption has decreased by 3.05% and the total NO_x emissions have reduced by 10.39%. When the sailing time constraint is considered, the fuel consumption has decreased by 1.97%, the NO_x emissions have decreased by 8.31%, and the sailing time has been shortened by 2.92%.

These findings demonstrate that the proposed optimization method can be applied not only to the multi-objective optimization of ship design parameters but also to the multi-objective optimization of ship operation. Furthermore, the method effectively enhances ship energy efficiency and reduces GHG and NO_x emissions. More importantly, this method will help reduce the ship's carbon footprint and provide shipowners with a feasible solution to relieve the pressure of upcoming carbon taxes and carbon emission regulations.

This study focuses on energy efficiency optimization based on the operational data of a single voyage, without accounting for the varying meteorological conditions and sea conditions encountered during actual ship operations. To be more in line with real-world sailing scenarios and meet the ongoing demand for global maritime decarbonization, future research will incorporate real-time meteorological data to develop a dynamic optimization model, further enhancing the effectiveness of ship energy efficiency optimization.

NOMENCLATURE

Symbol	Quantity Description
A_E/A_0	propeller area ratio [-]
A_F	maximum transverse area of the hull above the water surface [m^2]
B	breadth of ship [m]
d	draft of ship [m]
D	propeller diameter [m]

E_{NO_x}	NO_x emission rate [g/kWh]
h_s	significant wave height [m]
J	advance coefficient [-]
K_Q	torque coefficients of the propeller [-]
K_T	thrust coefficients of the propeller [-]
L_{PP}	length between perpendiculars [m]
n_p	propeller speed [rpm]
n_e	engine speed [rpm]
P/D	propeller pitch ratio [-]
P_e	main engine power [kW]
Q	propeller's torque [kNm]
R_{total}	total resistance in sea conditions [kN]
R_T	resistance in calm water [kN]
R_{wave}	added wave resistance in regular seas [kN]
R_{wind}	added wind resistance [kN]
S_0	total sailing distance [n mile]
t	thrust deduction coefficient [-]
T	sailing time [h]
T_e	propeller's effective thrust [kN]
u_C	advance velocity component [m/s]
V_s	Sailing speed [kn]
V_{wr}	relative wind speed [m/s]
β	heading angle[rad]
ω	frequency of encounter [-]
ω_e	frequency of encounter [Hz]
Z	Number of propeller blades [-]
η	propulsion efficiency [-]
η_0	open water efficiency of the propeller [-]
η_t	transmission efficiency [-]
η_S	transmission efficiency of the shaft [-]
ρ_a	the air density [kg/m^3]

Abbreviations

ALO	Ant Lion Optimization
BN	Beaufort wind scale
DWT	Deadweight Tonnage
EEDI	Energy Efficiency Design Index
EEOI	Energy Efficiency Operational Indicator
FOC	Fuel oil consumption
GHG	Greenhouse gas
IMO	International Maritime Organization
MCDM	Multi-criteria decision-making

NSGA-II	Non-dominated Sorting Genetic Algorithm II
NOx	Nitrogen oxide
PSO	Particle swarm optimization
RPM	Revolutions per minute
SEEMP	Ship Energy Efficiency Management Plan
SFOC	Specific fuel oil consumption
TOPSIS	The Technique for Order of Preference by Similarity to Ideal Solution

REFERENCES

[1] Sirimanne, S.N., Hoffman, J., Juan, W., Asariotis, R., Assaf, M., Ayala, G., Benamara, H., Chantrel, D., Hoffmann, J., and Premti, A. 2019. Review of maritime transport 2019. in United Nations conference on trade and development, Geneva, Switzerland.

[2] Tuswan, T., Sari, D.P., Muttaqie, T., Prabowo, A.R., Soetardjo, M., Murwantono, T.T.P., Utina, R., Yuniati, Y., 2023. Representative application of LNG-fuelled ships: a critical overview on potential GHG emission reductions and economic benefits. *Brodogradnja*, 74(1), 63-83. https://doi.org/10.21278/brod74104

[3] Inal, O. B., 2024. Decarbonization of shipping: Hydrogen and fuel cells legislation in the maritime industry. *Brodogradnja*, 75(2), 1-13. https://doi.org/10.21278/brod75205

[4] MEPC, R., 2023. 2023 IMO strategy on reduction of GHG emissions from ships.

[5] MEPC, R., 2022. 2022 GUIDELINES FOR THE DEVELOPMENT OF A SHIP ENERGY EFFICIENCY MANAGEMENT PLAN (SEEMP).

[6] Tokuşlu, A., 2020. Analyzing the Energy Efficiency Design Index (EEDI) performance of a container ship. *International Journal of Environment and Geoinformatics*, 7(2), 114-119. https://doi.org/10.30897/ijegeo.703255

[7] Bialystocki, N., Konovessis, D., 2016. On the estimation of ship's fuel consumption and speed curve: A statistical approach. *Journal of Ocean Engineering and Science*, 1(2), 157-166. https://doi.org/10.1016/j.joes.2016.02.001

[8] Sun, C., Wang, H., Liu, C., Zhao, Y., 2019. Dynamic prediction and optimization of energy efficiency operational index (EEOI) for an operating ship in varying environments. *Journal of Marine Science and Engineering*, 7(11), 402. https://doi.org/10.3390/jmse7110402

[9] Beşikçi, E.B., Keçeci, T., Arslan, O., Turan, O., 2016. An application of fuzzy-AHP to ship operational energy efficiency measures. *Ocean engineering*, 121, 392-402. https://doi.org/10.1016/j.oceaneng.2016.05.031

[10] Chi, H., Pedrielli, G., Ng, S.H., Kister, T., Bressan, S., 2018. A framework for real-time monitoring of energy efficiency of marine vessels. *Energy*, 145, 246-260. https://doi.org/10.1016/j.energy.2017.12.088

[11] Stanić, V., Hadjina, M., Fafandjel, N., Matulja, T., 2018. Toward shipbuilding 4.0-an industry 4.0 changing the face of the shipbuilding industry. *Brodogradnja*, 69(3), 111-128. https://doi.org/10.21278/brod69307

[12] Ma, L., Yang, P., Gao, D., Bao, C., 2023. A multi-objective energy efficiency optimization method of ship under different sea conditions. *Ocean Engineering*, 290, 116337. https://doi.org/10.1016/j.oceaneng.2023.116337

[13] Ren, L. Diao, Y., 2014. Matching optimization of ship engine propeller and net for the trawler based on genetic algorithm. 10th International Conference on Natural Computation (ICNC), IEEE, 19-21 August, Xiamen, China. https://doi.org/10.1109/ICNC.2014.6975906

[14] Li, Z., Wang, K., Hua, Y., Liu, X., Ma, R., Wang, Z., Huang, L., 2024. GA-LSTM and NSGA-III based collaborative optimization of ship energy efficiency for low-carbon shipping. *Ocean Engineering*, 312, 119190. https://doi.org/10.1016/j.oceaneng.2024.119190

[15] Mirjalili, S., 2015. The ant lion optimizer. *Advances in engineering software*, 83, 80-98. https://doi.org/10.1016/j.advengsoft.2015.01.010

[16] Tadros, M., Ventura, M., Soares, C.G., 2018. Optimization scheme for the selection of the propeller in ship concept design, in Progress in maritime technology and engineering, CRC Press, 233-239. https://doi.org/10.1201/9780429505294-27

[17] Esmailian, E., Ghassemi, H., Zakerdoost, H., 2017. Systematic probabilistic design methodology for simultaneously optimizing the ship hull–propeller system. *International Journal of Naval Architecture and Ocean Engineering*, 9(3), 246-255. https://doi.org/10.1016/j.ijnaoe.2016.06.007

[18] Taskar, B., Yum, K.K., Pedersen, E., Steen, S., 2015. Dynamics of a marine propulsion system with a diesel engine and a propeller subject to waves. 34th International conference on ocean, offshore and arctic engineering, 31 May-5 June, St. John's, Newfoundland, Canada. https://doi.org/10.1115/OMAE2015-41854

[19] Marques, C., Belchior, C., Caprace, J.-D., 2018. Optimising the engine-propeller matching for a liquefied natural gas carrier under rough weather. *Applied Energy*, 232, 187-196. https://doi.org/10.1016/j.apenergy.2018.09.155

[20] Lee, S.-M., Roh, M.-I., Kim, K.-S., Jung, H., Park, J.J., 2018. Method for a simultaneous determination of the path and the speed for ship route planning problems. *Ocean Engineering*, 157, 301-312. https://doi.org/10.1016/j.oceaneng.2018.03.068

[21] Li, X., Ding, K., Xie, X., Yao, Y., Zhao, X., Jin, J., Sun, B., 2024. Bi-objective ship speed optimization based on machine learning method and discrete optimization idea. *Applied Ocean Research*, 148, 104012. https://doi.org/10.1016/j.apor.2024.104012

[22] Chang, C.C., Chang, C.-H., 2013. Energy conservation for international dry bulk carriers via vessel speed reduction. *Energy Policy*, 59, 710-715. https://doi.org/10.1016/j.enpol.2013.04.025

[23] Lu, R., Turan, O., Boulougouris, E., Banks, C., Incecik, A., 2015. A semi-empirical ship operational performance prediction model for voyage optimization towards energy efficient shipping. *Ocean Engineering*, 110, 18-28. https://doi.org/10.1016/j.oceaneng.2015.07.042

[24] Norstad, I., Fagerholt, K., Laporte, G., 2011. Tramp ship routing and scheduling with speed optimization. *Transportation Research Part C: Emerging Technologies*, 19(5), 853-865. https://doi.org/10.1016/j.trc.2010.05.001

[25] Sahin, B., Soylu, A., 2020. Multi-layer, multi-segment iterative optimization for maritime supply chain operations in a dynamic fuzzy environment. *IEEE Access*, 8, 144993-145005. https://doi.org/10.1109/ACCESS.2020.3014968

[26] Theotokatos, G., Tzelepis, V., 2015. A computational study on the performance and emission parameters mapping of a ship propulsion system. *Proceedings of the Institution of Mechanical Engineers, Part M: Journal of Engineering for the Maritime Environment*, 229(1), 58-76. https://doi.org/10.1177/1475090213498715

[27] Fagerholt, K., Psaraftis, H.N., 2015. On two speed optimization problems for ships that sail in and out of emission control areas. *Transportation Research Part D: Transport and Environment*, 39, 56-64. https://doi.org/10.1016/j.trd.2015.06.005

[28] Yan, X., Wang, K., Yuan, Y., Jiang, X., Negenborn, R.R., 2018. Energy-efficient shipping: An application of big data analysis for optimizing engine speed of inland ships considering multiple environmental factors. *Ocean Engineering*, 169, 457-468. https://doi.org/10.1016/j.oceaneng.2018.08.050

[29] Wang, K., Yan, X., Yuan, Y., Li, F., 2016. Real-time optimization of ship energy efficiency based on the prediction technology of working condition. *Transportation Research Part D: Transport and Environment*, 46, 81-93. https://doi.org/10.1016/j.trd.2016.03.014

[30] Zheng, Z., Zhou, X., 2019. Design and simulation of ship energy efficiency management system based on data analysis. *Journal of Coastal Research*, 94(SI), 552-556. https://doi.org/10.2112/SI94-109.1

[31] Kalajdžić, M., Vasilev, M., Momčilović, N., 2023. Inland waterway cargo vessel energy efficiency in operation. Brodogradnja, 74(3), 71-89. https://doi.org/10.21278/brod74304

[32] Deb, K., Agrawal, S., Pratap, A., Meyarivan, T., 2000. A fast elitist non-dominated sorting genetic algorithm for multi-objective optimization: NSGA-II. Parallel Problem Solving from Nature PPSN VI: 6th International Conference Paris, France, September 18–20, Proceedings 6. Springer. https://doi.org/10.1007/3-540-45356-3_83

[33] Mirjalili, S., Dong, J.S., 2020, Multi-objective optimization using artificial intelligence techniques, *Springer*. https://doi.org/10.1007/978-3-030-24835-2

[34] Deb, K., Pratap, A., Agarwal, S., Meyarivan, T., 2002. A fast and elitist multiobjective genetic algorithm: NSGA-II. *IEEE transactions on evolutionary computation*, 6(2), 182-197. https://doi.org/10.1109/4235.996017

[35] Huang, C., Huang, H., Hang, P., Gao, H., Wu, J., Huang, Z., Lv, C., 2021. Personalized trajectory planning and control of lane-change maneuvers for autonomous driving. *IEEE Transactions on Vehicular Technology*, 70(6), 5511-5523. https://doi.org/10.1109/TVT.2021.3076473

[36] Dogan, O., Deveci, M., Canıtez, F., Kahraman, C., 2020. A corridor selection for locating autonomous vehicles using an interval-valued intuitionistic fuzzy AHP and TOPSIS method. *Soft Computing*, 24, 8937-8953. https://doi.org/10.1007/s00500-019-04421-5

[37] Yang, Z., Zhang, C., Ge, L., Gong, D., Gu, Y., Huang, T., 2014. Comprehensive fuzzy evaluation based on entropy weight method for insulator flashover pollution. *Electric Power Automation Equipment*, 34(4), 90-94.

[38] Ma, Q., Wang, Z., Zhou, T., Liu, Z., 2024. Robust optimization method of emergency resource allocation for risk management in inland waterways. *Brodogradnja*, 75(1), 1-22. https://doi.org/10.21278/brod75103

[39] MEPC, R., 2017. 2013 interim guidelines for determing minimum propulsion power to maintain the manoeuvrability of ships in adverse conditions.

[40] Holtrop, J., Mennen, G., 1982. An approximate power prediction method. *International shipbuilding progress*, 29(335), 166-170. https://doi.org/10.3233/ISP-1982-2933501

[41] ITTC, 2014. Guidelines–Speed and Power Trials, Part 2: Analysis of Speed. Power Trial data, 7.5-04.

[42] Gerritsma, J., Beukelman, W., 1972. Analysis of the resistance increase in waves of a fast cargo ship. *International shipbuilding progress*, 19(217), 285-293. https://doi.org/10.3233/ISP-1972-1921701

[43] Shigunov, V., 2018. Manoeuvrability in adverse conditions: Rational criteria and standards. *Journal of Marine Science and Technology*, 23(4), 958-976. https://doi.org/10.1007/s00773-017-0525-z

[44] Van Lammeren, W., van Manen, J.v., Oosterveld, M., 1969. The Wageningen B-screw series.

[45] Barnitsas, M.M., Ray, D., Kinley, P., 1981. KT, KQ and efficiency curves for the Wageningen B-series propellers, *University of Michigan*.

[46] Wang, K., Yan, X., Yuan, Y., Jiang, X., Lin, X., Negenborn, R.R., 2018. Dynamic optimization of ship energy efficiency considering time-varying environmental factors. *Transportation Research Part D: Transport and Environment*, 62, 685-698. https://doi.org/10.1016/j.trd.2018.04.005

[47] Kim, M., Hizir, O., Turan, O., Day, S., Incecik, A., 2017. Estimation of added resistance and ship speed loss in a seaway. *Ocean engineering*, 141, 465-476. https://doi.org/10.1016/j.oceaneng.2017.06.051